Quantum ferroelectricity in $K_{1-x}Na_xTaO_3$ and $KTa_{1-y}Nb_yO_3$

U. T. Höchli
IBM Zurich Research Laboratory,
8803 Rüschlikon, Switzerland

L. A. Boatner
*Solid State Division, Oak Ridge National Laboratory,**
Oak Ridge, Tennessee 37830
(Received 5 March 1979)

The effect known as ferroelectricity arises when forces between polarizable ions in a solid produce a spontaneous displacement of these ions which results in a lattice polarization below some characteristic (Curie) temperature. Fluctuations in this polarization may be thermally induced as in the case of classical ferroelectrics, or if the Curie temperature is near 0 K, the fluctuations can be due to quantum-mechanical zero-point motion. The term "quantum ferroelectric" is applied to those systems where fluctuations in the polarization result from the zero-point motion. Experimental determinations of variations in the dielectric constant, spontaneous polarization, and elastic compliance as a function of temperature and impurity concentration are reported for $K_{1-x}Na_xTaO_3$ and $KTa_{1-y}Nb_yO_3$, and these results show that the physical properties of quantum ferroelectrics differ from those of classical ferroelectrics in the following ways: First, for a quantum ferroelectric, the transition temperature depends on impurity concentration (i.e., on an effective order parameter) as $T_c \propto (x - x_c)^{1/2}$, as opposed to $T_c \propto (x - x_c)$ for the classical case. Second, the inverse dielectric constant varies with temperature as $\epsilon^{-1} \propto T^2$ for the quantum-mechanical case, instead of $\epsilon^{-1} \propto T$. Finally, the distribution of transition temperatures in a given macroscopic sample with a Gaussian impurity concentration distribution is $p(T_c) \propto T_c \exp(-\alpha T_c^4)$ for the quantum ferroelectric, as opposed to a Gaussian for the classical situation. These results are in agreement with previous theoretical predictions of some of the distinguishing characteristics of quantum ferroelectricity.

I. INTRODUCTION

Quantum-mechanical effects in ferroelectricity have been observed previously by Sawaguchi *et al.*,[1] who found that, at low temperature, the dielectric constant of $SrTiO_3$ did not obey the Curie-Weiss law but rather that it could be described by the following expression:

$$\epsilon - \epsilon_{T=\infty} = C[\tfrac{1}{2} T_1 \coth(T_1/2T) - T_0]^{-1} \ , \qquad (1)$$

where T_1 represents the dividing temperature between the quantum-mechanical and classical regions. This equation had been derived earlier by Barrett,[2] using a model based on a quantum-statistical ensemble of oscillators. More recently, Eq. (1) has been used to fit measurements of the dielectric constants of $KTaO_3$ under atmospheric[3] as well as applied isotropic[4] pressure. In spite of its apparent ability to provide a reasonable fit to this dielectric-constant data, Eq. (1) is in contradiction with the limiting behavior of $\epsilon(T \to 0)$ as predicted by the more recent quantum theoretical treatments[5–7] of incipient ferroelectrics with $T_c = 0$, as well as with the behavior predicted by the acoustic-optic mode-coupling model[8] which is applicable for low, but nonzero, critical temperatures. The variation of ϵ with temperature predicted in the more recent theoretical works is given by

$$\epsilon - \epsilon_{T=\infty} = B(T - T_c)^{-\gamma} \ , \qquad (2)$$

where $\gamma = 2$ (quantum theory) for $T_c = 0$ and $\gamma \approx 1.4 \pm 0.2$ (mode-coupling model) for temperatures up to ~ 100 K. The mode-coupling regime has been found to extend[9] to $T \approx 120$ K in the case of $SrTiO_3$.

In the classical temperature range Eqs. (1) and (2) become equivalent and $\gamma = 1$ in this region. The modern, self-consistent theories, therefore, predict that below a certain temperature, the Curie-Weiss law assumes the form given in Eq. (2) with $\gamma \approx 1.4$ and that, if $T_c = 0$, there is a third regime near $T = 0$ for

which $\gamma = 2$. In spite of the marked algebraic difference between Eqs. (1) and (2), we found that on a log-log plot an appropriate series of three straight lines in accordance with the three regimes of Eq. (2) can also approximate Eq. (1) to a surprisingly high degree of accuracy and that, consequently, it is necessary to obtain very precise data on a system with $T_c \sim 0$ in order to distinguish between the validity of the two equations. Accordingly, in order to determine the validity of the scaling argument in the quantum theory of ferroelectricity (leading to $\gamma = 2$) and the mode-coupling theory (leading to $\gamma \approx 1.4$), we have grown mixed crystals of $K_{1-x}Na_xTaO_3$ and $KTa_{1-y}Nb_yO_3$ with critical temperatures as low as possible, and have carefully measured the dielectric response for these systems. These data were fit to both Eqs. (1) and (2); an evaluation of the fitting parameters in terms of the respective models, together with the quality of the fit, has enabled us to discriminate in favor of the self-consistent theories and against the older quantum oscillator theory.

The manner in which the phase boundary approaches the quantum limit $T_c = 0$ has also been predicted by the self-consistent theories and previous experiments[10] on the system $KTa_{1-y}Nb_yO_3$ have confirmed these predictions. In the present work, comparisons will be made between the earlier data for $KTa_{1-y}Nb_yO_3$ and the new data presented here for $K_{1-x}Na_xTaO_3$. In spite of the apparent differences between these two cases (in the perovskite system ABO_3 an A ion is replaced by an isoelectric impurity in one case, and a B ion is replaced in the other), the two phase diagrams scale perfectly. These observations further reinforce the understanding of the apparently dominant role of oxygen polarizability in the ferroelectric behavior of the perovskite oxides.[11]

Ferroelectrics with T_c in the quantum range (quantum ferroelectrics) are characterized by some additional peculiar features which are of more practical interest: When metal contacts are applied, deep space-charge layers develop[12] which may be reinforced by external bias fields. This feature, together with high coercive fields of $\sim 10^6$ V/m, can prevent an accurate determination of the spontaneous polarization by conventional techniques. We have therefore resorted to cooling the sample through the transitions using only a moderate bias field (2×10^5 V/m). The polarization is found to relax sufficiently slowly to permit a measurement of the piezoelectric coefficient[13] by the ultrasonic resonance method. Near the quantum limit, T_c is extremely sensitive to crystal composition and this effect has been used to measure the distribution of Na (Nb in the previous experiments) concentration within a given sample. The impurity distributions are checked against the impurity profile obtained from x-ray fluorescence measurements and provide a test for the consistency of the data.

II. EXPERIMENTAL

In a classical ferroelectric, the spontaneous polarization in the low-temperature phase varies with temperature as

$$P \propto (T_c - T)^{1/2} , \tag{3}$$

and the dielectric constant is governed by the following relation:

$$\epsilon \propto |T - T_c|^{-1} . \tag{4}$$

Therefore, by plotting P^2 or ϵ^{-1} vs T, it is generally quite easy to determine the critical temperature T_c. In quantum ferroelectrics, however, only approximate and, in part, conflicting expressions exist for $P(T)$ and $\epsilon(T)$; therefore, a determination of T_c is not so straightforward. In addition, measurements of the ferroelectric characteristics of mixed-crystal quantum ferroelectrics pose some particular problems. First, mixed crystals are generally somewhat inhomogeneous and this leads to a distribution of Curie temperatures within the sample. The response of a given ferroelectric parameter near T_c must be convoluted with a measured or assumed distribution of Curie points in order to determine the true phase diagram and the true critical indices. Other difficulties arise from the high coercive field at low temperature which slows down switching of the spontaneous polarization and accordingly prevents its determination in terms of released charge. The formation of strong space-charge layers is a further detriment in making hysteresis measurements. Since an application of the classical methods to determine T_c, P_s, and ϵ for quantum ferroelectrics leads to somewhat inconsistent results, we shall specify in detail by what methods these characteristic quantities have been measured here as a function of sample composition and temperature.

A. Sample characterization and determination of inhomogeneities

The mixed-crystal specimens investigated here were grown according to the method described by Wemple.[14] A mixture consisting of Ta_2O_5, K_2CO_3, Na_2CO_3, and minute traces of CuO powder was heated to 1450 C in a Pt crucible and then cooled at rates from 2 to 20 C/hr. Clear crystals of $\sim \frac{1}{4}$ cm^3 were obtained from 300 g ingots, and the sample composition was determined by x-ray fluorescence microprobe analysis. The average Na concentration corresponded closely to the composition of the starting powder, and the inhomogeneity was typically several percent of the average concentration near the surface of a single-crystal ingot. Attempts to grow identical crystals with different growth runs led to a

composition which was reproducible to within about $\Delta x = 0.02$. A higher Na content generally resulted in decreased quality.

For the highest concentration of Na ($x = 0.28$), the inhomogeneity is of the order of 5% absolute Na concentration ($\Delta x \approx 0.05$) and therefore T_c spreads over a range of about 6 K. Lower concentrations are characterized by lower inhomogeneities, but since the transition line in the phase diagram becomes steeper near $T_c = 0$, the spread of T_c increases as the quantum limit is approached.

B. Elastic response near distributed Curie points

Determination of the Curie point rests on a measurement of some critical response and a fit of the results to a theoretical expression. Three main difficulties arise in this procedure near the quantum limit:

(i) There are only approximate expressions available for the dielectric constant and the polarization.

(ii) The Curie point is distributed in a sample that is not completely homogeneous, and the associated distributions of x, ϵ, p, and s are approximately known. (The distribution in the composition may be determined by microprobe analysis, however.)

(iii) In general, there is no way of uniquely predicting how the responses superimpose in a system with distributed critical temperatures. Fortunately, for the purpose of determining T_c the problem of a superposition of responses in inhomogeneous samples has been solved for the particular case of the elastic compliance. A microscopic[15,16] mean-field theory predicts that the elastic compliance is described by a step function

$$s = s_a \quad \text{for} \quad T < T_c \ , \tag{5}$$

$$s = s_c \quad \text{for} \quad T \geq T_c \ , \tag{6}$$

where s_a and s_c are the elastic compliances in the axial and cubic phases, respectively. This discontinuous change is attributed to the abrupt change of symmetry at T_c. Below T_c the symmetry is sufficiently low to allow linear coupling between some strain waves and soft modes, while above T_c the symmetry is high enough to prevent such interactions. This model was initially formulated for the case of $SrTiO_3$ which is characterized by an elastic step function[17–19] smeared out by a few degrees and superimposed on a weak divergence. While the actual limiting width in this case may be ~ 0.5 K,[17] in many samples the true width is much greater and may be attributed to some type of sample imperfection.

In $KTa_{1-y}Nb_yO_3$, the elastic step width varies from sample to sample but is consistent with the sample inhomogeneity as determined by electron microprobe analysis. This observation[10] prompted a systematic study of the influence of inhomogeneity on elastic behavior.

A sample with a sharply-defined T_c has an elastic compliance which, according to the theory based on the $SrTiO_3$ model,[15] depends on temperature as shown in Fig. 1. If a single-crystal sample is driven into a length-extensional vibration, its resonance frequency occurs at

$$f_{res} = (2l)^{-1}(\rho_m s)^{-1/2} \ , \tag{7}$$

where ρ_m is the mass density, l is the sample length, and s is the elastic compliance. The resonance frequency is characterized by an impedance minimum which may be determined using a conventional bridge method. Now consider a sample with T_c varying along an axis of vibration labeled x. The strain will be $S_{xx} = s_a T_{xx}$ for those parts of the crystal with $T_c > T$, and $S_{xx} = s_c T_{xx}$ for those parts with $T_c < T$. Here s_a and s_c are as defined for Eqs. (5) and (6), and T_{xx} is the stress provided by the transverse electrostrictive effect. If $p(T_c)$ denotes the probability that a given T_c will occur, then the total strain is given by

$$S_{xx} = T_{xx}\left[s_a + \int p(T_c)\, dT_c (s_a - s_c)\right] \ .$$

The effective elastic compliance thus becomes

$$s_{11} = s_c + \int_T^\infty p(T_c)(s_a - s_c)\, dT_c \ . \tag{8}$$

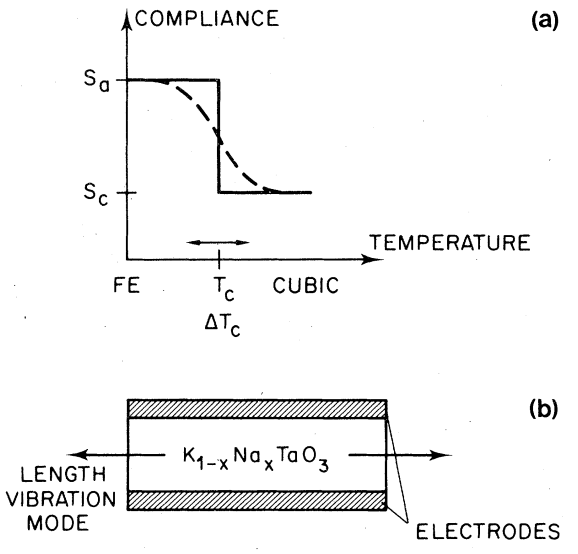

FIG. 1. (a) Elastic compliance as a function of temperature. The solid line shows the variation expected for a sharp, homogeneous phase transition. The broken line indicates the variation at a diffuse transition. (b) Vibrational mode used to determine s_{11}.

This convolution of the elastic step function by a distribution of critical temperatures is particularly simple [much more so than the convolution of a Curie-Weiss expression, $|T-T_c|^{-1}$, or of a polarization function, $(T_c-T)^{1/2}$]. This simplicity provided the motive for studying inhomogeneity by acoustic resonance rather than by dielectric constant or spontaneous polarization measurements. It can now be assumed that the Na concentration x (or Nb concentration y) is distributed log normally,[10] i.e., that the probability p that some concentration is present locally in the sample is given by

$$p(x)=(a/\pi)^{1/2}\exp[-a(x-x_0)^2] \ , \tag{9}$$

x_0 being the mean concentration.

In the classical limit where T_c depends linearly on x,[20,21] identical distributions result for T_c and for x, in which case the elastic compliance was shown[10] to depend on temperature as

$$s_{11}(T)=\tfrac{1}{2}(s_a+s_c) + \tfrac{1}{2}(s_a-s_c)\,\mathrm{erf}\{a(T-T_c)\} \ . \tag{10}$$

In the quantum limit, the phase diagram is nonlinear; therefore, a two-step procedure was devised in order to determine both the homogeneity and the effective Curie point of the sample. In the first step, the measured elastic compliances were fit to the *best* error function in order to determine T_c approximately. Then a plot of T_c (approximate) vs x was fit to $(x-x_c)^{1/\Phi}$. The critical concentration was determined by recognizing that, at the quantum limit, exactly one-half of the sample is ferroelectric at 0 K and therefore the elastic step is reduced to one-half of its value in the classical limit. The fit of T_c (approximate) to $(x-x_c)^{1/\Phi_0}$ yielded $\Phi_0\approx 2$ for both $K_{1-x}Na_xTaO_3$ and $KTa_{1-y}Nb_yO_3$. With this value of Φ_0, a better than log-normal approximation for the distribution of T_c was found, by inserting $T_c=\alpha^{-1/2}(x-x_c)^{1/2}$ into Eq. (9),

$$p(T_c)\,dT_c=(\text{const})\,T_c\exp-[\alpha a T_c^2+a(x_c-x_0)]^2 \ . \tag{11}$$

This expression reduces to

$$p(T_c)\,dT_c\propto T_c\exp-\alpha^2a^2T_c^4 \tag{12}$$

for $x_c=x_0$. The convolution of a step function with distributions of this type cannot be given in a closed form, so the data were fit by numerical methods. The result is shown in Fig. 2 for $K_{1-x}Na_xTaO_3$. As can be seen in this figure, for some samples the assumed distribution fits the data very well, while for others there are slight deviations on the wings of the curves.

Some deviations may also be attributed to a dip of the elastic constants near T_c superimposed on the step function. Such dips are presumably indicative of the breakdown of mean-field theory. This suggestion is based on the predictions of a theory of critical elastic response in $SrTiO_3$. Since experimental evidence for a dip in $KTaO_3$ compounds is scarce, no attempt of its analysis was made.

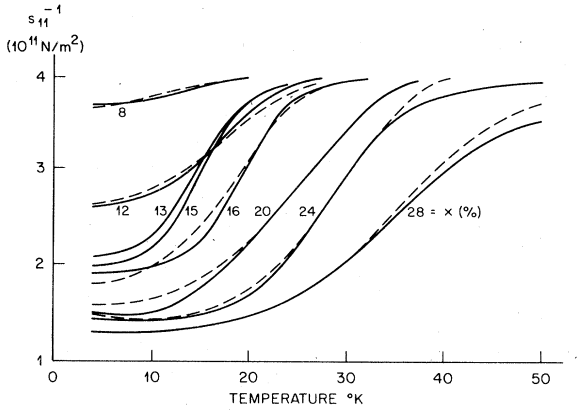

FIG. 2. Elastic compliance (solid lines) and the fit to computed curves (broken lines) for eight samples of $K_{1-x}Na_xTaO_3$. The curves are labeled by the sodium concentration x in percent. The broken curves were computed assuming that the transition was broadened by compositional inhomogeneity.

C. Determination of the phase diagram from elastic and dielectric data

When the transition temperatures obtained from a fit with the distributions discussed above (i.e., T_c from the second iteration) were again fit to $(x-x_c)^{1/\Phi}$, the result $\Phi=2.1\pm0.2$ was well within the error associated with Φ_0 from the first iteration; and therefore, it was pointless to iterate the value of the distribution any further. The phase diagram for the quantum-ferroelectric region of the solid solution $K_{1-x}Na_xTaO_3$ is shown in Fig. 3, where it is apparent that $T_c\propto(x-x_c)^{1/2.1}$ fits the data consistently and that the crossover between quantum ($\Phi=2$) and classical ($\Phi=1$) ferroelectricity occurs in a temperature range between 15 and 50 K. Figure 3 also includes two data points of Davis[22] which were obtained from dielectric susceptibility measurements.

The data for the system $KTa_{1-y}Nb_yO_3$ are analogous to those for $K_{1-x}Na_xTaO_3$ and yielded a value of $\Phi=1.8\pm0.3$. In $KTa_{1-y}Nb_yO_3$ a comparison was made between the homogeneity determined by electron microprobe analysis, and that determined acoustically. The results are shown in Table I, where it is seen that the standard deviation of y is the same whether it is determined acoustically or by mi-

TABLE I. Electromechanical properties of $KTa_{1-y}Nb_yO_3$ for $y < 0.05$. Method of determination: *a*—electron probe, *b*—elastic step, *c*—hysteresis *P* vs *E* at 2.5 mHz, *d*—capacitance vs temperature at 10 kHz.

Nb concentration			Polarization[a] at 0 K	Inverse dielectric constant at 0 K	Transition Temperature		
Mean	Standard deviation				Mean		Standard deviation
a	*a*	*b*	*c*	*d*	*d*	*b*	*b*
Percent	percent	percent	10^{-3} C/m^2	10^{-4}			
0				2.3	...		
0.25				1.3	...		
0.8	<0.3	0.3	2	0.5	...	0	13
1.4	<0.2	0.2	13	1.0	20	21.2	4.4
1.7	<0.2	0.3	31	1.4	23	27.5	4.6
2.8	0.3	0.4	42	3.5	33	36.4	3.6
3.0	0.4	0.3	42	5.9	47	45.6	3.8
4.6	1.5	~1	55	7.9	60	56	12

[a]Reference 10.

croprobing, and that it increases continuously with the mean concentration. Table I also lists the values of P_s and ϵ^{-1} at 0 K which were used to determine β and γ [defined by $P_x \sim (x - x_c)^\beta$ and $\epsilon^{-1} \sim (x - x_c)^\gamma$, respectively] and provides the data necessary for a comparison between the transition temperatures as obtained from acoustic measurements and from the maximum of the dielectric constant. If it is assumed that the uncertainty of T_c (acoustic) is one-fifth of the standard deviation due to sample inhomogeneity, then most of the "dielectric" critical temperatures are at variance with the critical temperatures as determined acoustically. From this we conclude that the convolution of $\epsilon(T)$ with a non-Gaussian distribution does not have its maximum at T_c as predicted by the Curie-Weiss law. The determination of a nonlinear phase diagram from dielectric measurements appears to pose stricter requirements on sample homogeneity than does an evaluation by the acoustic method.

The system $K_{1-x}Na_xTaO_3$ is presently less suitable for such a comparison: The sample quality is somewhat inferior to that of $KTa_{1-y}Nb_yO_3$, (probably because of the large Na concentration) and the resolution of the Na fluorescence appears to be poorer than that for Nb. The dielectric constant shows no notable dispersion. After the samples are cooled to 4 K, it drifts[23] considerably, especially in samples with a low critical temperature.

In $K_{0.87}Na_{0.13}O_3$, the dielectric constant drops from 51 000 to 44 000 in the first hour after cool-down (aging). After this time period, the drift becomes much smaller. Since the aging time of one hour is comparable to the discharge time of pure $KTaO_3$ after the application of an electric field,[12,23] it is tempting to attribute aging to the spontaneous formation of space charge following rapid cool-down. With increasing dielectric constants, the Debye length $l_0 = (\epsilon\epsilon_0 V_B/ne)^{1/2}$, V_B being the barrier height, and thus the region of charge depletion can become comparable to the same dimensions. The associated Poisson field acts as a bias to reduce the effective capacitance. To test this hypothesis, the capacitance was measured simultaneously using the acoustic flexure-

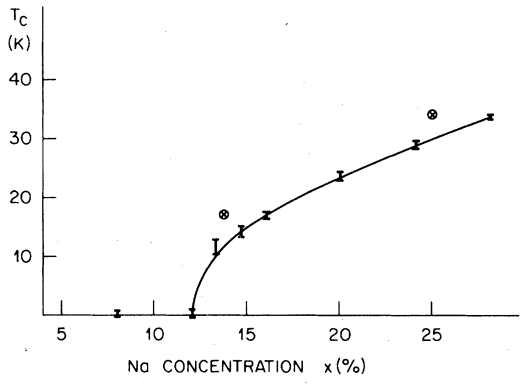

FIG. 3. Phase diagram of $K_{1-x}Na_xTaO_3$ near the quantum limit. This experimental curve is to be compared with the theoretical result given in Fig. 1 of Ref. 6.

resonance technique[12] in several samples after cool-down. From the flexure resonance, the space-charge density and the mechanical quality factor of the sample can be deduced; the results are shown in Table II. The evidence is against spontaneous dielectric saturation for the following reasons:

(i) The Poisson field $|E| = 2$ kV/m as measured by flexure resonance accounts for a change $\Delta\epsilon/\epsilon$ in the order of $+10^{-3}$. This is different in sign and magnitude from the measured $\Delta\epsilon/\epsilon \sim -10^{-1}$.

(ii) The Poisson field does not increase in time. The fact that no flexure resonance is observed immediately after cool-down should be attributed to the initial low mechanical quality factor.

(iii) The mechanical quality factor increases gradually with time. This leads to an alternate suggestion, namely, that dielectric aging is due to a mechanical stress release which occurs after cool-down. The average stress which would have to be released to account for the observed $\Delta\epsilon/\epsilon$ is of the order[23] of 4×10^3 N/m^2. This corresponds to a strain of $\sim 2 \times 10^{-8}$. These values are quite reasonable, but a quantitative means of supporting the stress-release hypothesis has not been found, and we are unable to explain why $\Delta\epsilon/\epsilon$ is always negative while ϵ depends linearly on stress. Since aging has no influence on the Poisson field, all data have been reported for the case of thermodynamic equilibrium. The results for the dielectric constants are illustrated in Fig. 4. The solid lines through the data of Fig. 4 result from attempts to theoretically describe the behavior of the susceptibility near the quantum limit. They are discussed in Sec. III.

TABLE II. Dielectric constant ϵ, space-charge density ρ, and mechanical quality factor Q, as a function of time after rapid cool-down to 4 K.

TIME minutes	ϵ	ρ C/m^3	Q
0	513 50	. . .	. . .
5	490 20	. . .	. . .
12	472 50	0.83	100
15	469 80	1.25	180
25	465 70	1.04	200
45	460 30	0.98	540
60	447 80	1.14	520

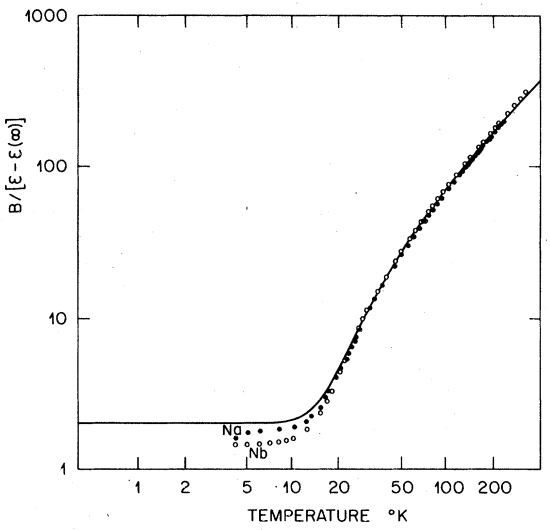

FIG. 4. The critical part of the inverse dielectric constant in $KTa_{0.992}Na_{0.008}O_3$ (open circles) and $K_{0.88}Na_{0.12}TaO_3$ (solid circles). $B/[\epsilon(T) - \epsilon(\infty)]$ is shown along with the fit to $(T - T_c)^{-\gamma}$ in the three temperature ranges: 15 to 35 K, 35 to 80 K, and above 80 K.

D. Spontaneous polarization and piezoelectric effect

The spontaneous polarization is customarily measured from hysteresis loops. At low temperatures, however, the coercive field necessary to switch the polarization exceeds 1 MV/m. Such fields induce large amounts of space charge which obscure the charge stored by lattice polarization. We have therefore determined P_s from the piezoelectric effect.[13]

The piezoelectric constant d_{31} which couples the strain in the x direction to the polarization in the z direction can be written

$$d_{31} = 2 g_{31} P_s \ , \tag{13}$$

where g_{31} is the electrostrictive constant valid for both phases at temperatures sufficiently close to T_c. The piezoelectric constant was determined by acoustic resonance of a polarized sample in the ferroelectric phase, while the electrostrictive constant required a resonance measurement in the dielectric phase under suitable dc bias. The appropriate formulas[12,13,17] are

$$d_{31} = k (s_{11}/\epsilon\epsilon_0)^{1/2} \ , \tag{14}$$

$$g_{31} = k/(\epsilon\epsilon_0)^{3/2} l f \rho_m^{1/2} E_{\text{bias}} \ , \tag{15}$$

where k is the piezoelectric coupling factor obtained from the characteristics of the impedance cycle

[see Fig. 5(a)],

$$k = [1 + 16\pi^{-1}(G_{max} - G_{min})^{-1} \times (f_1 - f_2)^{-1} C f_0^2]^{-1/2} , \quad (16)$$

where f_1 and f_2 are the frequencies at which $G = \frac{1}{2}(G_{max} + G_{min})$. The impedance cycle [Fig. 5(b)] may cross the abscissa at frequencies f_r and f_a, called the resonance and antiresonance frequencies, respectively. These frequencies are determined by balancing the sample with the bridge with C set at zero. In this case

$$k + \tfrac{1}{4}\pi^2[(f_a - f_r)^2/f_0^2 + Q^{-2}]^{1/2} . \quad (17)$$

For large Q, Eq. (17) approached the form given in the piezoelectric standards.[24]

Since it is not necessary for the polarization to be switched in these experiments, only low E fields are required and the sample may be cooled through the transition while biased. This ensures that the space-charge fields induced by the bias are relatively low and that the induced polarization is rather homogeneous.

A measure of the homogeneity of the polarization is obtained from the characteristics of the flexure resonance. For an approximately homogeneous space-charge distribution, the difference in polarization from surface to surface is described[12] by

$$\Delta P = (3s/\epsilon\epsilon_0)^{1/2} k_F/g , \quad (18)$$

where k_F is the piezoelectric coupling factor of the flexure resonance. This gives a measure of the reliability for the determination of P_s by means of the piezoelectric effect. After removal of the domain structure by a transient biasing field, the polarization is given by

$$P_s = (s/\epsilon\epsilon_0)^{1/2} k_L/2g , \quad (19)$$

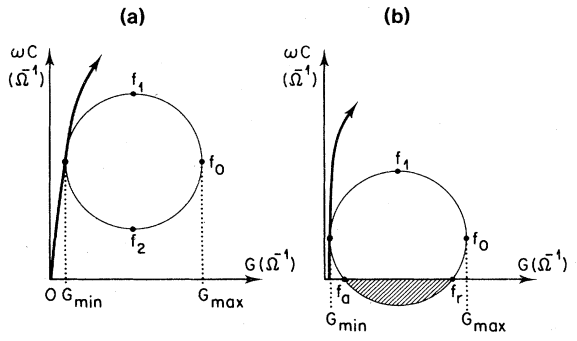

FIG. 5. Real vs imaginary parts of dielectric constant near an acoustic resonance. Weak resonances are handled according to Ref. 13. For strong resonances with an inductive region (shaded), the piezoelectric constant is determined as indicated in the text.

k_L being the piezoelectric coupling factor for the length-extensional resonance. Measurements for P_s as summarized in Table I have an uncertainty of the order of $\Delta P \sim 1$ mC/m^2 arising from field-induced space charge.

III. MICROSCOPIC MODELS OF INCIPIENT FERROELECTRICS

The earliest available data for an incipient ferroelectric are based on capacitance measurements as a function of temperature. From such measurements it was usually found that $\epsilon^{-1} \propto |T - T_c|$ both above and below the phase transition. Such a result can be explained by a Devonshire-like expansion of the free energy in powers of the free (homogeneous) polarization and temperature. Barrett[22] was the first to recognize the influence of quantum effects on the dielectric constant, and he developed an expression for the susceptibility of an ensemble of anharmonic oscillators coupled only by the requirement that they obey Bose statistics. The result was Eq. (1), which for $T >> T_1$ coincides with the Curie-Weiss law. His predictions were confirmed[1] in $SrTiO_3$ and the parameters T_1 and T_0 were determined by an experimental fit. Barrett's expression approximately fits the experimental curves for $KTaO_3$ under pressure, as well as the data for the mixed crystals in the present paper. His model, which neglects all explicit interactions among oscillating Ta dipoles and between Ta dipoles and the lattice, was not capable of explaining the significance of the parameters T_1, however. By taking the interaction between dipoles into account, Pytte[16] was able to predict the occurrence of a step discontinuity in the elastic constants, to reproduce Barrett's result, and to explain T_1 in terms of the interaction parameters introduced in his model. He also pointed out that the Barrett expression is only correct if the soft optic-mode frequency is large compared with the acoustic frequencies. Obviously, this assumption breaks down if the optic mode becomes soft in the quantum region, e.g., sufficiently close to the quantum limit of a ferroelectric. For this limit, a prediction has recently been made by Schneider *et al.*[6] and Morf *et al.*[5] These authors consider the influence of quantum fluctuations on the phase diagram and on the expectation value of the order parameter, and they adopt a Hamiltonian of the form

$$H = \sum_{L,\alpha} \frac{P_{L\alpha}^2}{2M} + \tfrac{1}{2}A \sum_{L\alpha} X_{L\alpha}^2 + \frac{B}{4n} \sum_{L} \left[\sum_{\alpha} X_{L\alpha}^2 \right]^2 - C \sum_{L,L',\alpha} X_{L'\alpha}^2 X_{L\alpha}^2 . \quad (20)$$

Here L denotes lattice sites and $\alpha = 1, \ldots, n$ denotes spatial directions. When applied to the system

$K_{1-x}Na_xTaO_3$, in the spirit of the Slater[25] model of ferroelectrics, the terms are identified as the kinetic energy of the Ta atoms (being the displacement of the Ta ion), their harmonic and anharmonic binding to the rigid oxygen atoms, and their nearest-neighbor Ta-Ta interaction, respectively. An interaction parameter given by

$$S = 2CZ_n - A \tag{21}$$

is defined, where Z_n is the number of nearest neighbors, and it is shown that the transition line separating the cubic from the ferroelectric phase is governed by

$$T_c \propto (S - S_c)^{1/2} , \tag{22}$$

S_c being defined as the interaction parameter for which T_c vanishes. Similarly, the polarization at $T = 0$ is given by

$$P \propto (S - S_c)^{1/2} . \tag{23}$$

Additionally, the inverse dielectric constant at $T = 0$ is given by

$$\epsilon^{-1} \propto S - S_c , \tag{24}$$

and, at $S = S_c$ with T variable,

$$\epsilon^{-1} \propto T^2 . \tag{25}$$

The interaction parameter in this case has a particularly simple form since the Hamiltonian contains only one nearest-neighbor interaction term. Morf *et al.*[5] have also shown that the critical dimensionality which limits the mean-field behavior is raised by one in the presence of zero-point motion, and also if long-range forces are included. Classical critical indices such as those given by Eqs. (22)–(25) should therefore apply to quantum ferroelectrics down to two dimensions, although at $d = 2$ (and only there) logarithmic corrections are expected.

We may now assume that: (i) both the harmonic binding and the dipolar interaction change linearly with the lattice distance, and (ii) that the lattice distance is a linear function of the Na content (at least between 15 and 30% Na). Then S is proportional to the Na content x and Eqs. (22)–(24) are valid if S and S_c are replaced by x and x_c, respectively. The identification of S with x in $K_{1-x}Na_xTaO_3$ is straightforward, whereas in $KTa_{1-y}Nb_yO_3$ the Nb content not only changes the average but also the local interaction parameters of the crucial B site. The lack of experimental evidence for randomness is attributed to the long range of the dipolar forces which average out local variations of dipolar occupancy. The data are now checked against the set of Eqs. (22)–(25) and Eq. (2). The inverse dielectric constant has historically[2,3] been fit to Eq. (1), which is at variance with Eq. (2) at the quantum limit. Figure 4, however, shows data for ϵ^{-1} at the quantum limit, along with a fit to Eq. (2) in the three temperature regimes. The fit to Eq. (1) is not shown here, since it is hardly distinguishable from the fit to Eq. (2) on this plot. Only a careful evaluation of the parameters resulting from least-squares fits allows one to exclude the fit to Eq. (1) as "unphysical."[26] A fit of ϵ^{-1} to Eq. (2) yields $\gamma = 2.1$ for the lowest temperature regime only for the two samples at the quantum limit. This is in accordance with the predictions of Eq. (25). Between the quantum-limit regime and about 120 K, and at all temperatures up to 120 K for the near-quantum-limit samples, the data fit the equation $\epsilon^{-1} \propto (T - T_c)^{\gamma}$ with $\gamma \approx 1.4$. (Such behavior was previously observed[27] and attributed[9,11] to coupling between acoustic and soft modes.) Above 120 K, the Curie-Weiss law holds and $\gamma = 1$.

The fits of dielectric constants to power laws are only slightly better than those of Eq. (1). Their main merit is the one-to-one correspondence of critical exponents with phenomena governing the dielectric susceptibility, as summarized in Table III.

The Curie point T_c as determined from elastic measurements (Fig. 3) was fit to Eq. (22); data from Abel[4] are included in this figure. The fit is as good as that obtained[10] for $KTa_{1-y}Nb_yO_3$ and serves to confirm the predictions of the quantum-limit theory.

TABLE III. Critical exponents for the susceptibility.

Phenomenon	Exponent γ in $\epsilon^{-1} = (T - T_c)^{\gamma}$	
	γ_{theor}	γ_{exp}
Each Ta atom responds to $E_{ext} + \langle \sum E_{int} \rangle$ (mean-field theory)	1	1.1
Ta couples to acoustic modes of same frequency (up to 60 cm^{-1})	1.4	1.4
Each Ta atom responds to fields of other Ta atoms self-consistently	2	2.1

IV. COMPOSITIONAL INHOMOGENEITY OF MIXED CRYSTALS AND THE QUANTUM LIMIT

A realization of quantum-limit conditions required the preparation of mixed crystals. The composition of mixed crystals inevitably varies within a given sample, since it is extremely difficult to maintain a constant composition of the feed liquid during crystal growth. The inhomogeneities as determined in this work are on the order of several percent of the nominal concentration over a 1 cm sample length. These inhomogeneities prevented us from improving on the precision of the critical indices for P_s and ϵ [Eqs. (23) and (24)]. Data for $\epsilon(x,T)$ are shown in Fig. 6. The data for $K_{1-x}Na_xTaO_3$ are inferior to those for $KTa_{1-y}Nb_yO_3$ in this respect; the Na concentration of $x=0.12$ at the quantum limit entails a large standard deviation of x. An improvement in the sample homogeneity would substantially contribute to quantum-limit investigations.

The chance of finding a cubic single crystal closer to the quantum limit than $SrTiO_3$ and $KTaO_3$ appears to be quite small. If we assume that the interaction parameters are randomly distributed in nature, then in the classical limit the Curie temperatures are evenly distributed and the probability of finding a Curie point between T_c and T_c+dT_c is given by

$$p(S)\,dS = p(T_c)\,dT_c = \text{const} \approx 0.6/\text{deg K (see Ref. 28)} \quad . (26)$$

In the quantum limit

$$S \propto T_c^2\,, \quad dS = 2T_c\,dT_c\,, \tag{27}$$

and the distribution of Curie points becomes

$$p(T_c)\,dT_c = 0.012\,T_c/\text{deg K}\quad . \tag{28}$$

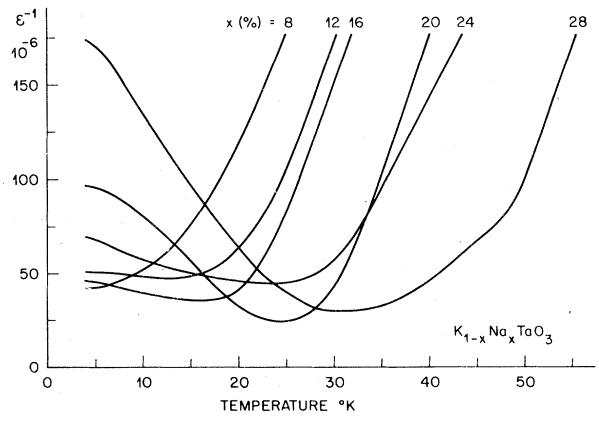

FIG. 6. Dielectric constants of $K_{1-x}Na_xTaO_3$ as a function of temperature for several values of x. The curves are labeled by the value of x in percent.

[The constant 0.012 was determined by equating $p(T_c)$ of Eqs. (26) and (28) at the crossover from quantum to classical behavior near 50 K.] The probability of finding a single crystal at the quantum limit vanishes because, at that limit, the sensitivity of T_c to the interaction parameter diverges. Its sensitivity to composition also diverges and this enhances the requirements on the homogeneity for a given maximum spread of the transition. As an example, the quantum limit of $K_{1-x}Na_xTaO_3$ is at $x=0.12$. Above this concentration, $T_c \approx 17(x-x_c)^{1/2}$. Attempts to reproduce crystals identically with a set concentration generally leads to differences of about 2%. At the quantum limit this corresponds to about 25 K on the phase diagram. With present-day crystal-growth techniques, the production of crystals which are homogeneous on the T_c scale exactly at the quantum limit is very difficult.

Inhomogeneous samples still give rise to acoustic resonances with reasonably high quality factors (about 1000 at 0 K), and their elastic compliance can be used to determine both T_c and its distribution $p(T_c)$ which may vary from Gaussian in the classical region to a distribution

$$p(T_c)\,dT_c = bT_c \exp[-(T_c/a)^4]$$

in the quantum limit. This distribution has a secondary maximum at a temperature $T \approx a$ which should not be interpreted as a transition temperature of the bulk material.

V. CONCLUSION

We have shown experimentally that, under a certain condition, quantum fluctuations can suppress the ferroelectric phase as has been suggested on theoretical grounds. The condition is that the interaction parameter, which is a weighted difference between the dipolar interaction and the harmonic binding of the dipole to the oxygen lattice, falls into a narrow range between the values given by the classical and the quantum-mechanical displacive limits. Of the two ternary single crystals which come under this category, i.e., $SrTiO_3$ and $KTaO_3$, the latter is the only example devoid of complications arising from a structural phase transition to D_4 symmetry while remaining in the paraelectric phase. The results presented here show that substituting Na for K removes the suppression of ferroelectricity and that above the critical concentration of 12% Na ($x=0.12$), $K_{1-x}Na_xTaO_3$ is ferroelectric at 0 K. At this critical concentration, the transition line $T_c(x)$ terminates with a vertical tangent, and critical indices have been found which correspond to a Gaussian fixed point for a four-dimensional isotropic system. That this should be the case has been shown for a

one-, for a two- and for an (unphysical) ∞-dimensional order parameter. While no rigorous proof seems to be available for $n=3$, we have shown here on experimental grounds, that the three-dimensional order-parameter "polarization" in $KTaO_3$-type compounds qualifies for a Gaussian fixed point at the quantum limit. The transition line is described by

$$T_c \propto (S - S_c)^{1/\phi}, \quad \phi = 2 \quad . \tag{29}$$

The inverse dielectric constant depends on S as

$$\epsilon_S^{-1} \propto (S - S_c)^{\gamma_S}, \quad \gamma_S = 1 \quad , \tag{30}$$

and on T as

$$\epsilon_T^{-1} \propto T^{\gamma_T}, \quad \gamma_T = 2 \quad , \tag{31}$$

as deduced from the scaling equation[5] $\gamma_T/\gamma_S = \phi$. This last exponent is compatible with the experimental data for ϵ^{-1} near $T=0$.

The findings are qualitatively the same for $K_{1-x}Na_xTaO_3$ and $KTa_{1-y}Nb_yO_3$. Both Na and Nb enhance the interaction parameter linearly with concentration. It is interesting to note that there is no qualitative difference between the nature of the effects associated with these two impurities in $KTaO_3$ even though they reside at different sites. This indicates that the influence of Na and Nb on $KTaO_3$ is not restricted to a particular site but must be of longer range. This view is in agreement with that put forward recently on the basis of Raman-scattering data: the large polarizability and eventual condensation in perovskites is due to the (anisotropic) polarizability of the oxygen shell which depends parametrically on the surrounding ions.[11] Incipient ferroelectrics are not restricted to the perovskite structure: KH_2PO_4 shows a phase diagram[29] under pressure which in all likelihood is due to the presence of a quantum limit.

ACKNOWLEDGMENTS

It is our pleasure to acknowlege stimulating discussions with Professor K. A. Müller, Professor J. Lajzerowicz, and Dr. T. Schneider, and correspondence with Professor A. Aharony. Special thanks are due to Dr. Philippe-André Buffat for performing the microprobe analysis of the Na-doped samples, and to Mr. D. Rytz for performing several numerical fits to the data.

---

*Operated by Union Carbide Corporation under Contract No. W-7405-eng-26 with the U. S. Department of Energy.

[1]E. Sawaguchi, A. Kikuchi, and Y. Kodera, J. Phys. Soc. Jpn. 17, 1666 (1962).
[2]J. H. Barrett, Phys. Rev. 86, 118 (1952).
[3]G. A. Samara and B. Morosin, Phys. Rev. B 8, 1256 (1973).
[4]W. R. Abel, Phys. Rev. B 4, 2696 (1971).
[5]R. Morf, T. Schneider, and E. Stoll, Phys. Rev. B 16, 462 (1977).
[6]T. Schneider, H. Beck, and E. Stoll, Phys. Rev. B 13, 1123 (1976).
[7]R. Oppermann and H. Thomas, Z. Phys. B 22, 387 (1975).
[8]H. Bilz, R. Migoni, G. Meissner, and K. A. Müller (unpublished).
[9]K. A. Müller and H. Burkard, Phys. Rev. B 19, 3593 (1979).
[10]U. T. Höchli, H. Weibel, and L. A. Boatner, Phys. Rev. Lett. 39, 1158 (1977). A fourth-power sign is missing on the T_c exponent of Eq. (7) of this reference. See Eq. (12).
[11]R. Migoni, H. Bilz, and D. Bäuerle, Phys. Rev. Lett. 11, 1155 (1976).
[12]U. T. Höchli and L. A. Boatner, J. Phys. C 10, 4319 (1977).
[13]E. J. Huibregste, W. H. Bessey, and M. E. Drougard, J. Appl. Phys. 30, 899 (1959).
[14]S. H. Wemple, Phys. Rev. A 137, 1575 (1965).
[15]J. C. Slonczewski and H. Thomas, Phys. Rev. B 1, 3599 (1970).
[16]E. Pytte, Phys. Rev. B 5, 3758 (1972).
[17]G. Rupprecht and W. H. Winter, Phys. Rev. 155, 1019 (1966).
[18]D. Bäuerle and W. Rehwald, Solid State Commun. 27, 1343 (1978).
[19]K. K. Murata, Phys. Rev. B 13, 4015 (1976).
[20]C. H. Perry, R. R. Hayes, and N. E. Tornberg, in *Molecular Spectroscopy of Dense Phases,* edited by S. G. Elkomoss (Elsevier, Amsterdam, 1976), p. 267.
[21]A. S. Chaves, F. C. S. Barreto, and L. A. A. Ribeiro, Phys. Rev. Lett. 37, 618 (1976).
[22]T. G. Davis, Phys. Rev. B 5, 2530 (1972).
[23]H. Uwe and T. Sakudo, J. Phys. Soc. Jpn. 38, 183 (1974).
[24]E. Hafner, Proc. IEEE 57, 179 (1969).
[25]J. C. Slater, Phys. Rev. 78, (1950).
[26]D. Rytz and U. T. Höchli (unpublished).
[27]H. Kind and K. A. Müller, Commun. Phys. 1, 223 (1976).
[28]This figure was deduced from the total number of ferroelectrics in a 1000 K range. E. Sawaguchi, in *Landbolt-Börnstein; Numerical Data and Functional Relationships in Science and Technology,* edited by K. H. Hellwege and A. M. Hellwege (Springer, Berlin, 1969), Group III, Vol. 3, p. 41.
[29]G. A. Samara, Ferroelectrics 7, 221 (1974).